MAGNETIC DESIGN OF ACCELERATOR MAGNETS

Arnaud Devred
CEA/Saclay

Technology School on Superconducting Magnets
Snowmass, CO
18 July 2001

Contents

- **Notations**
- **Field Computations for Simple Current Line Distributions**
- **Cosθ and Cos2θ Coil Designs**
- **Iron Yoke Contribution**
- **Operating Current Margin**
- **Other Designs**

Contents

- **Notations**
- Field Computations for Simple Current Line Distributions
- Cosθ and Cos2θ Coil Designs
- Iron Yoke Contribution
- Operating Current Margin
- Other Designs

Conductors Parallel to *z*-Axis

- Let $(O, \vec{x}, \vec{y}, \vec{z})$ designate a rectangular coordinate system, and let us a consider an ensemble of conductors parallel to the *z*-axis and uniform in z.

- The magnetic flux density, $\vec{B}$, produced by such current distribution can be shown to be parallel to the $(\vec{x}, \vec{y})$ plane and uniform in *z*

$$\vec{B} = B_{x}(x, y)\vec{x} + B_{y}(x, y)\vec{y}$$

where B_x and B_y are the *x*- and *y*- components of $\vec{B}$.

Complex Magnetic Flux Density

- Let **s** designate the complex variable variable defined

$$\mathbf{s} = x + i\, y$$

and let us introduce the complex magnetic flux density density, **B**, defined as

$$\mathbf{B(s)} = B_y(x,y) + i\, B_x(x,y)$$

- It can be derived from Maxwell's equations that, outside the conductors, **B** is a single-valued analytic function of **s**.

- Note that this property is only valid for the above definition of **B** and does not apply to $[B_x(x,y) + i\, B_y(x,y)]$.

Multipole Expansion (1/2)

- Let R_i designate the minimum distance between the conductors and the z-axis and let Γ_i designate the disk of center O and of radius R_i.

- The analytic function **B** can be expanded into a Taylor's series around the disk origin

$$\mathbf{B(s)} = \sum_{n=0}^{+\infty} \mathbf{B^{(n)}(0)}\, \frac{\mathbf{s}^n}{n!} \qquad \text{for } |\mathbf{s}| < R_i$$

where $\mathbf{B^{(n)}}$ designate the n-th derivative of **B** with respect to **s**.

Multipole Expansion (2/2)

- It is customary to re-write the previous power series expansion under the form.

$$\mathbf{B(s)} = \sum_{n=1}^{+\infty} \left(B_n + i\, A_n\right) \left(\frac{\mathbf{s}}{R_{ref}}\right)^{n-1} \qquad \text{for } |\mathbf{s}| < R_i$$
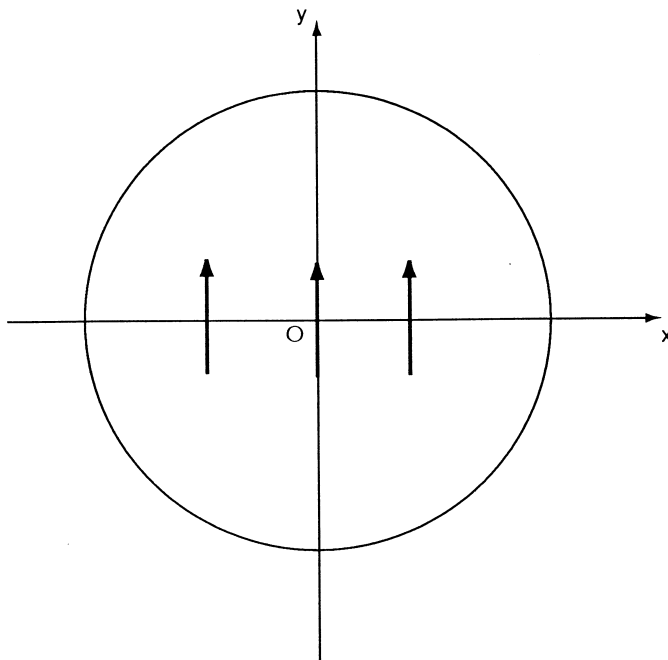
where R_{ref} is a so-called *reference radius*, and B_n and A_n are real and constant coefficients related to $\mathbf{B^{(n-1)}(0)}$ by

$$B_n + i\, A_n = \frac{\mathbf{B^{(n-1)}(0)}}{(n-1)!} R_{ref}^{\,n-1} \qquad \text{for } n, n \geq 1$$

Dipole Field Coefficients (1/3)

- Let us first consider a magnet such, that in the series expansion of **B**, all coefficients are nil except B_1.
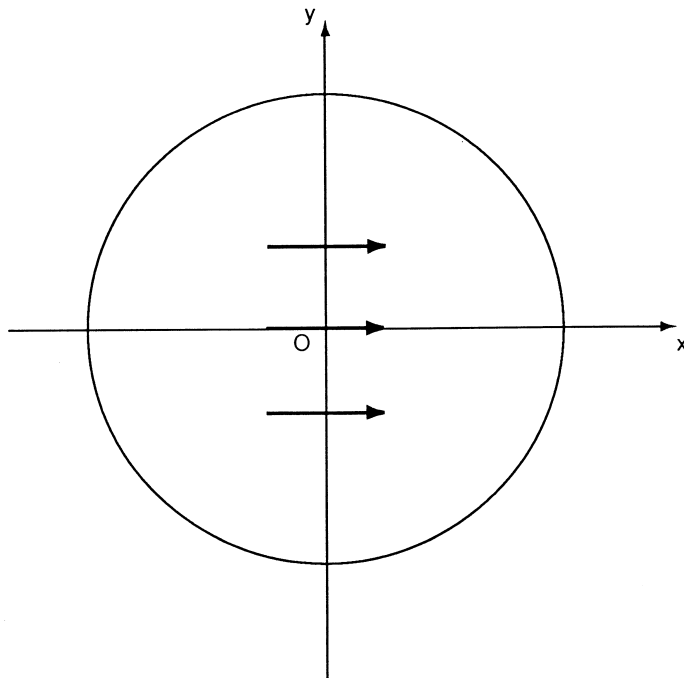
- Then we have

$$\mathbf{B(s)} = B_y + i\, B_x = B_1$$

- The magnetic flux density produced by such a magnet is uniform and vertical.

- It corresponds to a pure normal dipole magnetic flux density with a pole axis parallel to the y-axis.

8

Dipole Field Coefficients (2/3)

- Let us now consider a magnet such, that in the series expansion of **B**, all coefficients are nil except A_1.

- Then we have

$$\mathbf{B(s)} = B_y + i\, B_x = i\, A_1$$

- The magnetic flux density produced by such a magnet is uniform and horizontal.

- It corresponds to a so-called pure skew dipole magnetic flux density, with a pole axis rotated by an angle $(-\pi/2)$ with respect to the y-axis.

Dipole Field Coefficients (3/3)

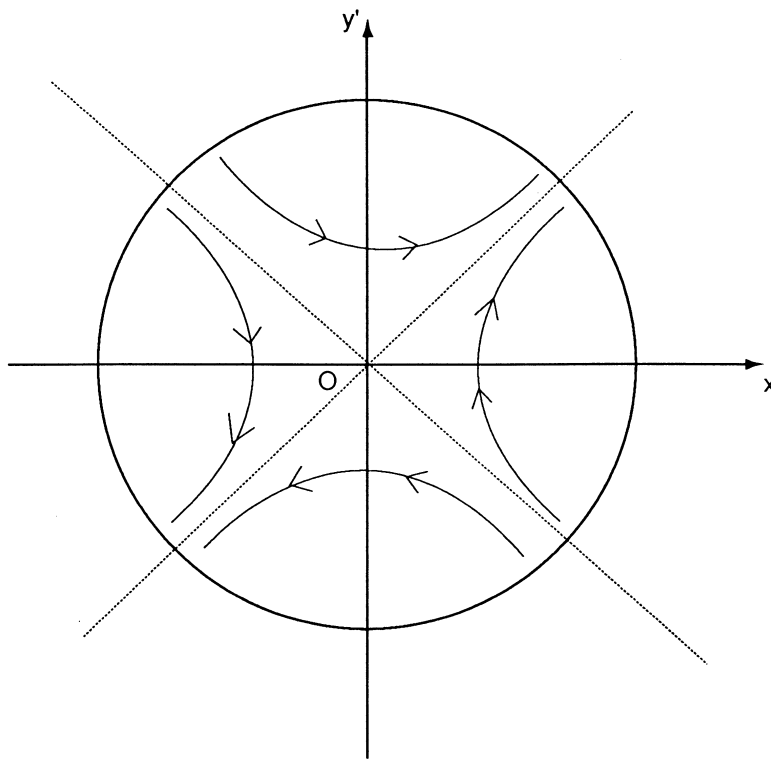- B_1 and A_1 are referred to as *normal and skew dipole field coefficients.*

Quadrupole Field Coefficients (1/4)

- Let us now consider a magnet such, that in the series expansion of **B**, all coefficients are nil except B_2.
- Then we have

$$\mathbf{B} = B_\mathrm{y} + \mathrm{i}\, B_\mathrm{x} = \frac{B_2}{R_\mathrm{ref}}\left(x + \mathrm{i}\, y\right)$$

- The y-component of the magnetic flux density produced by such a magnet is proportional to x, while the x-component is proportional to y, and the proportionality coefficients are the same.

Quadrupole Field Coefficients (2/4)

- It corresponds to a pure normal quadrupole magnetic flux density, with pole axes parallel to the first and second bisectors.
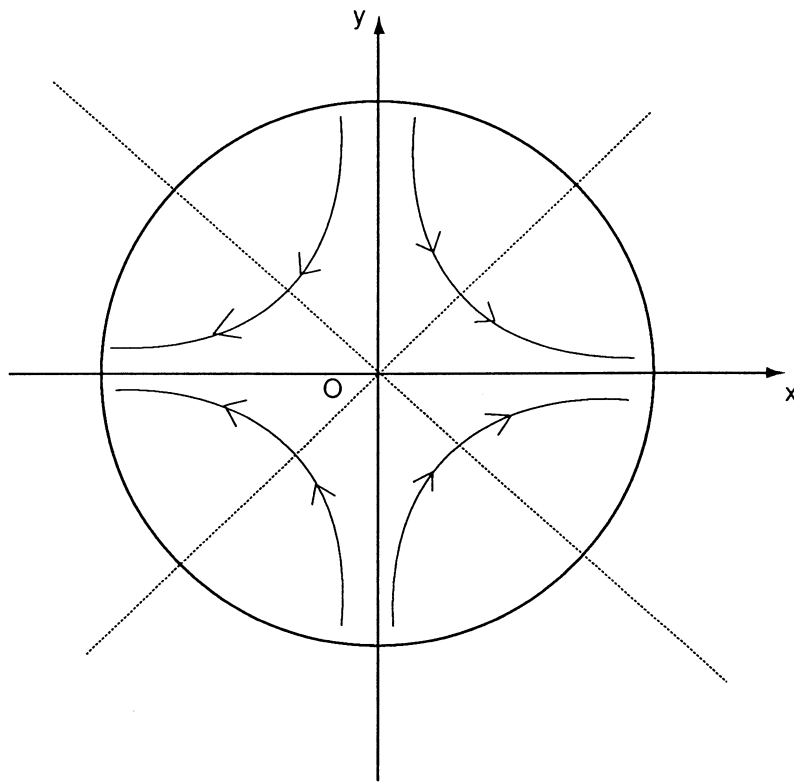
- The quadrupole field gradient, g, is simply

$$g = \frac{B_2}{R_{\text{ref}}}$$

Quadrupole Field Coefficients (3/4)

- Let us now consider a magnet such, that in the series expansion of **B**, all coefficients are nil except A_2.
- Then, we have

$$\mathbf{B} = B_{\mathrm{y}} + \mathrm{i}\, B_{\mathrm{x}} = \frac{A_2}{R_{\mathrm{ref}}}\left(-y + \mathrm{i}\, x\right)$$

Quadrupole Field Coefficients (4/4)

- This corresponds to a so-called skew quadrupole magnetic flux density, with pole axes rotated by an angle ($-\pi/4$) with respect to the first and second bisectors.

- B_2 and A_2 are referred to as *normal and skew quadrupole field coefficients.*

2N-Pole Field Coefficients

- Similarly to the case $n = 1$ and $n = 2$ and, it can be shown that the coefficients B_n and A_n correspond to pure $2n$-pole magnetic flux densities, and that the pole axes associated with A_n are rotated by an angle $[-\pi/(2n)]$ with respect to those associated with B_n.

- B_n and A_n are referred to as *normal and skew 2n-pole field coefficients.*

Reference Radius

• The reference radius is usually chosen so as to correspond to the region of space where the field must have good quality for beam optics reasons.
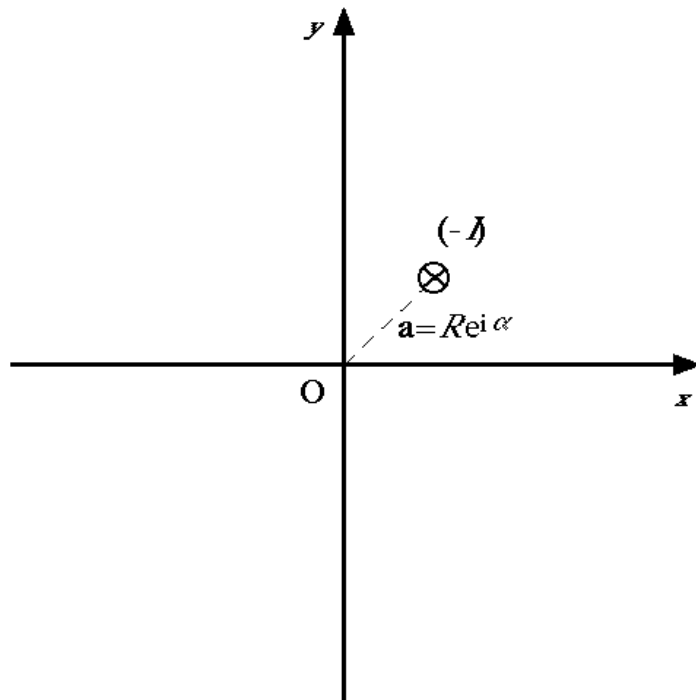
Example: for LHC, R_{ref} is set to 17 mm.

Contents

- **Notations**
- **Field Computations for Simple Current Line Distributions**
- **Cosθ and Cos2θ Coil Designs**
- **Iron Yoke Contribution**
- **Operating Current Margin**
- **Other Designs**

Single Current Line (1/4)

- let us consider a current line of intensity *(-I)*, parallel to the *z*-axis, and crossing the $(O, \vec{x}, \vec{y})$ plane at a point **a** = $R\,e^{i\theta}$ different from O.

- It is easy to derive that the complex magnetic flux density, **B**, produced by this current line is given by

$$\mathbf{B(s)} = -\frac{\mu_0 I}{2\pi}\frac{1}{\mathbf{s-a}}$$

where μ_0 is the magnetic permeability of vacuum.

18

Single Current Line (2/4)

- The above expression can easily be expanded into a power series

$$\mathbf{B(s)} = \sum_{n=1}^{+\infty} \left(B_n + i\, A_n \right) \left(\frac{\mathbf{s}}{R_{\text{ref}}} \right)^{n-1} \qquad \text{for } |\mathbf{s}| < |\mathbf{a}|$$
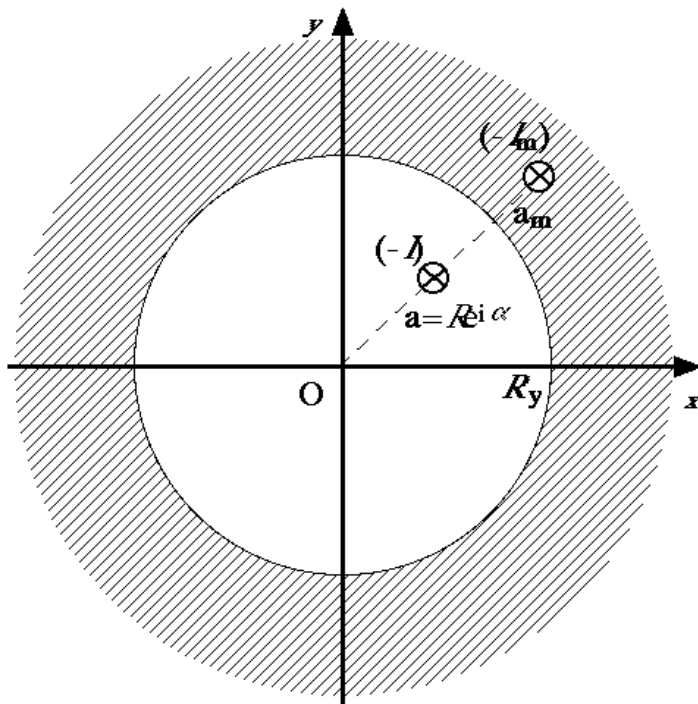
where B_n and A_n are given by

$$B_n + i\, A_n = \frac{\mu_0 I}{2\pi R_{\text{ref}}} \left(\frac{R_{\text{ref}}}{R} \right)^{n} \left[\cos(n\alpha) - i \sin(n\alpha) \right]$$

- Note that all multipole field coefficients are non zero.

Lecture IV

Single Current Line (3/4)

• Let us assume that the above current line is located within a ferromagnetic yoke of relative permeability, μ, and of inner radius, R_y.

• The yoke contribution can be shown to be the same as that of an image current line of intensity $(-I_m)$ located at a position $\mathbf{a_m}$ where

$$I_m = \frac{\mu-1}{\mu+1}I \quad \text{and} \quad \mathbf{a_m} = \frac{R_y^2}{\mathbf{a}^*}$$

Here, $\mathbf{a}^*$ is the complex conjugate of $\mathbf{a}$.

Single Current Line (4/4)

- Then, the multipole field coefficients for the current line with iron yoke, $B_n^{\text{w.y.}}$ and $A_n^{\text{w.y.}}$, are given by
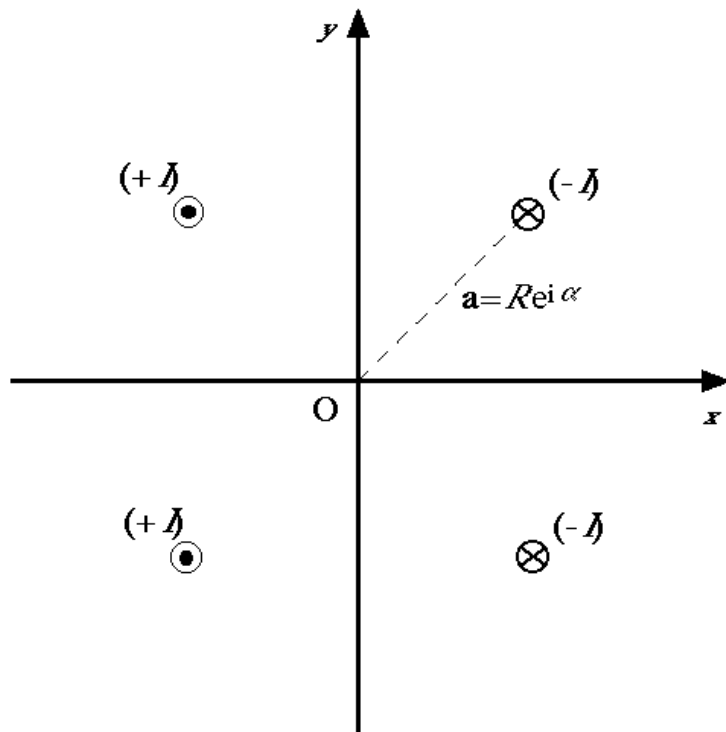
$$\frac{B_n^{\text{w.y.}} + i\, A_n^{\text{w.y.}}}{B_n^{\text{w/o.y.}} + i\, A_n^{\text{w/o.y.}}} = 1 + \frac{\mu - 1}{\mu + 1}\left(\frac{R}{R_y}\right)^{2n}$$

where $B_n^{\text{w/o.y.}}$ and $A_n^{\text{w/o.y.}}$ are the coefficients for the current line alone in free space.

- Note that the smaller R_y, the larger the enhancement.

Quadrupolet of Current Lines (1/2)

• Let us know consider a quadrupolet of current lines with an even symmetry with respect to the x-axis and an odd symmetry with respect to the y-axis.

• The magnetic flux density produced by this quadruplet can be computed by summing the contributions from each current line.

Quadrupolet of Current Lines (2/2)

- We get

$$\mathbf{B(s)} = \sum_{k=0}^{+\infty} B_{2k+1} \left(\frac{\mathbf{s}}{R_{\text{ref}}} \right)^{2k} \qquad \text{for } |\mathbf{s}| < R$$
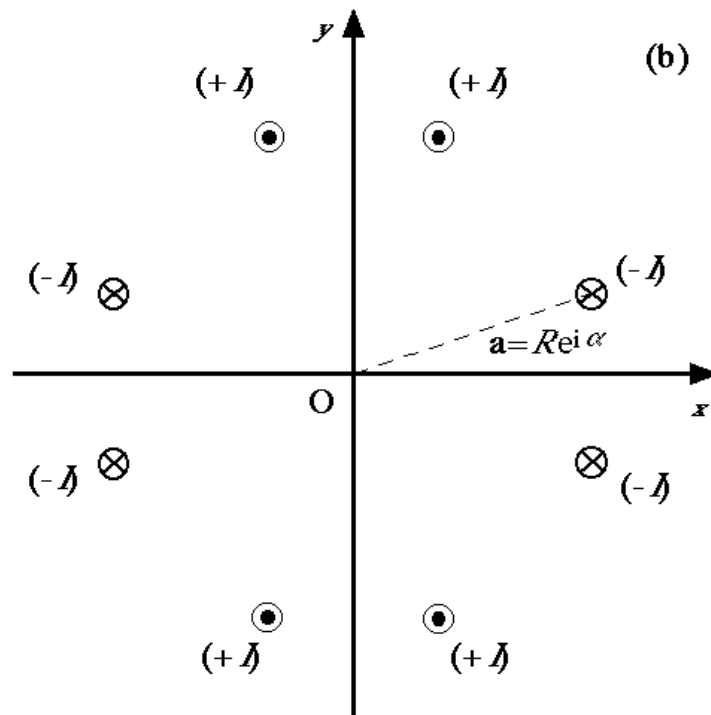
where

$$B_{2k+1} = \frac{2\mu_0 I}{\pi R_{\text{ref}}} \left(\frac{R_{\text{ref}}}{R} \right)^{2k+1} \cos\left[(2k+1)\alpha \right]$$

- The first term (k=0) corresponds to a pure normal dipole field parallel to the y-axis.

- The B_{2k+1} coefficients are called the *allowed* multipole field coefficients for this current distribution.

Octuplet of Current Lines (1/2)

- Let us finally consider an octuplet of current lines with an even symmetry with respect to the x- and y-axes and an odd symmetry with respect to the first and second bisectors.

- As for the quadruplet, the magnetic flux density can be computed by summing the contributions from each current line.

24

Octuplet of Current Lines (2/2)

- We get

$$\mathbf{B}(\mathbf{s}) = \sum_{k=0}^{+\infty} B_{4k+2} \left(\frac{\mathbf{s}}{R_{\mathrm{ref}}} \right)^{4k+1} \qquad \text{for } |\mathbf{s}| < R$$

where

$$B_{4k+2} = \frac{4\mu_0 I}{\pi R_{\mathrm{ref}}} \left(\frac{R_{\mathrm{ref}}}{R} \right)^{4k+2} \cos\left[(4k+2)\alpha \right]$$

- The first term (k=0) corresponds to a pure normal quadrupole field with pole axes parallel to the first and second bisectors.

- For this distribution, the *allowed* multipole field coefficients are the normal 2($4k$ +2)-pole field coefficients.

Summary

- Basic symmetries of current distribution suitable for dipole field production are: even symmetry with respect to x-axis and odd symmetry with respect to y-axis.

- Basic symmetries of current distribution suitable for quadrupole field production are: even symmetry with respect to x- and y-axes and odd symmetry with respect to first and second bisectors.

- Most superconducting accelerator magnet designs follow these symmetries.

Contents

- **Notations**
- **Field Computations for Simple Current Line Distributions**
- **Cosθ and Cos2θ Coil Designs**
- **Iron Yoke Contribution**
- **Operating Current Margin**
- **Other Designs**

Cos($p\theta$) Current Sheet (1/2)

- Let us consider a cylindrical current sheet of radius R, carrying a linear current density of the form

$$[-j_{sheet} \cos(p\theta)]$$

where j_{sheet} is a constant (in A/mm).

- The magnetic flux density produced inside the cylinder can be computed by dividing the sheet into elementary current lines of intensity

$$[-j_{sheet} R \cos(p\theta)] \, d\theta$$

and by integrating the current line contributions between O and (2π).

Cos($p\theta$) Current Sheet (2/2)

- Hence, we have

$$B_n + \mathrm{i}\,A_n = \frac{\mu_0 J_{\text{sheet}}}{2\pi}\left(\frac{R_{\text{ref}}}{R}\right)^{n-1}\left[\int_0^{2\pi} d\theta\,\cos(p\theta)\cos(n\theta) - \mathrm{i}\int_0^{2\pi} d\theta\,\cos(p\theta)\sin(n\theta)\right]$$

- The integration yields

$$B_n = A_n = 0 \quad \text{for } n \neq p \qquad B_p = \frac{\mu_0 J_{\text{sheet}}}{2} \quad \text{and} \quad A_p = 0$$

- It appears that a cos($p\theta$) current sheet produces a pure *normal* 2p-pole field.

Sin($p\theta$) Current Sheet

- Similarly, let us consider a cylindrical current shell with a linear current distribution of the form

$$[J_{\text{sheet}} \sin(p\theta)]$$

- Here, the multipole field coefficients of the magnetic flux density produced inside the cylinder are given by

$$B_n = A_n = 0 \quad \text{for } n \neq p \qquad B_p = 0 \quad \text{and} \quad A_p = \frac{\mu_0 J_{\text{sheet}}}{2}$$
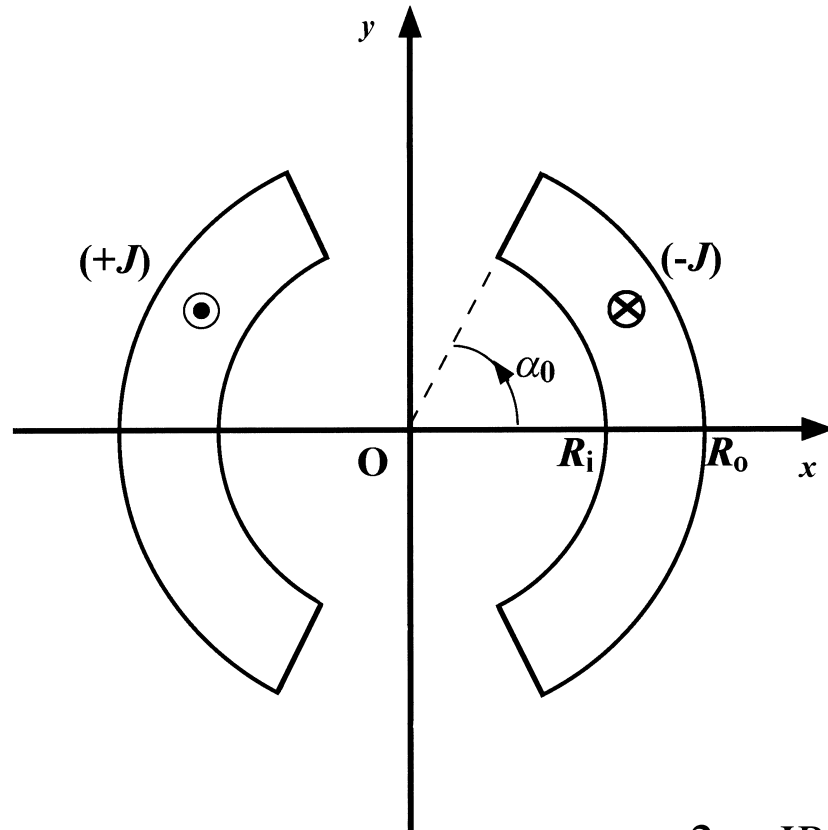
- Hence, a sin($p\theta$) current sheet produces a pure *skew* 2p-pole field.

Cos(θ) and Cos(2θ) Coil Designs

• Most dipole or quadrupole magnets rely on coil geometries, which, in the magnet cross-section, approximate a cos(θ) or a cos(2θ) current distribution.

• The approximation is based on cylindrical current shells of suitable symmetry.
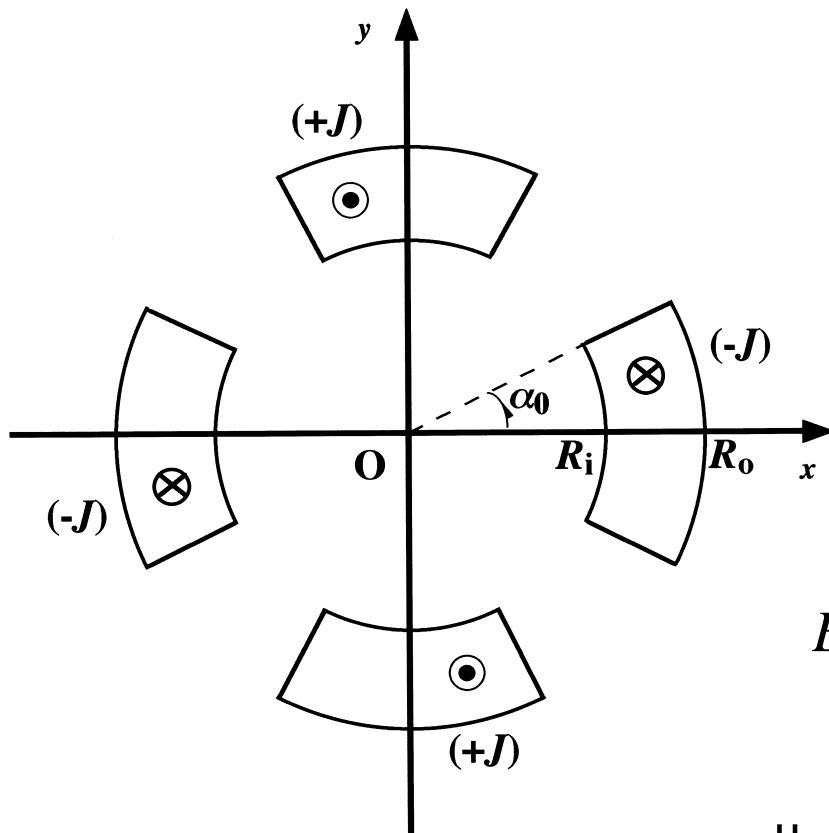
Cos(θ) Coil Design

• The multipole field coefficients produced in the coil aperture are

$$B_1 = \frac{2\mu_0 J}{\pi} (R_o - R_i) \sin(\alpha_0)$$

$$B_{2k+1} = \frac{2\mu_0 J R_{ref}}{\pi(2k+1)(2k-1)} \left[\left(\frac{R_{ref}}{R_i} \right)^{2k-1} - \left(\frac{R_{ref}}{R_o} \right)^{2k-1} \right] \sin[(2k+1)\alpha_0]$$
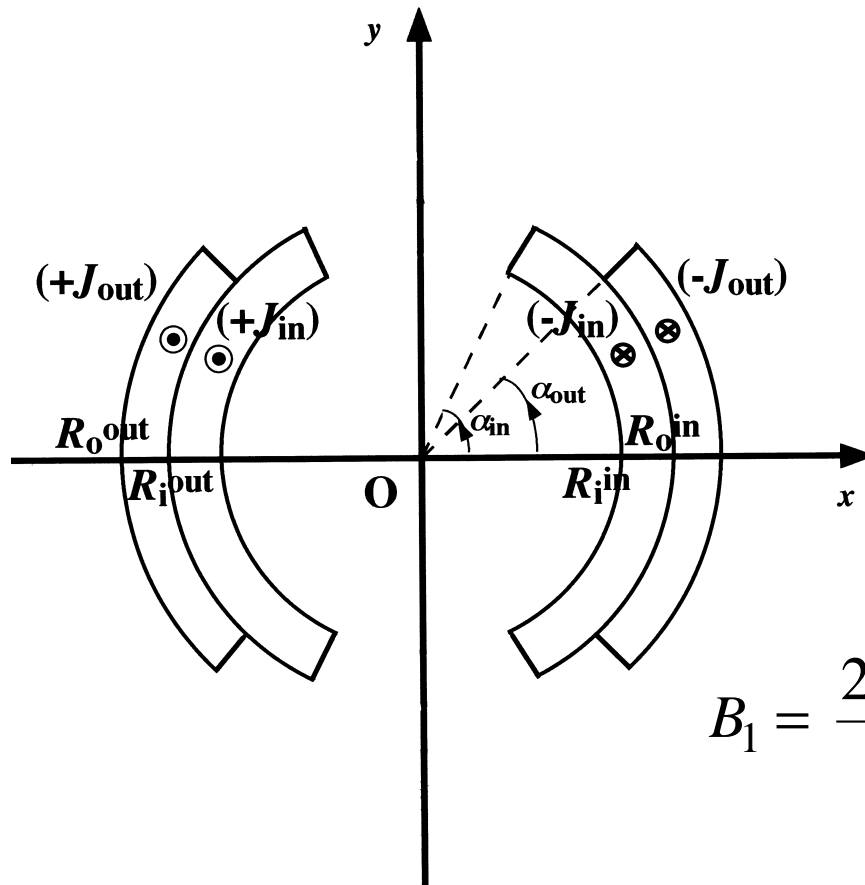
Cos(2θ) Coil Design

- The multipole field coefficients produced in the coil aperture are

$$B_2 = g \ R_{\text{ref}} = \frac{2\mu_0 J R_{\text{ref}}}{\pi} \ln\left(\frac{R_o}{R_i}\right) \sin(2\alpha_0)$$

$$B_{4k+2} = \frac{\mu_0 J R_{\text{ref}}}{\pi k(4k+2)} \left[\left(\frac{R_{\text{ref}}}{R_i}\right)^{4k} - \left(\frac{R_{\text{ref}}}{R_o}\right)^{4k}\right] \sin\left[(4k+2)\alpha_0\right]$$
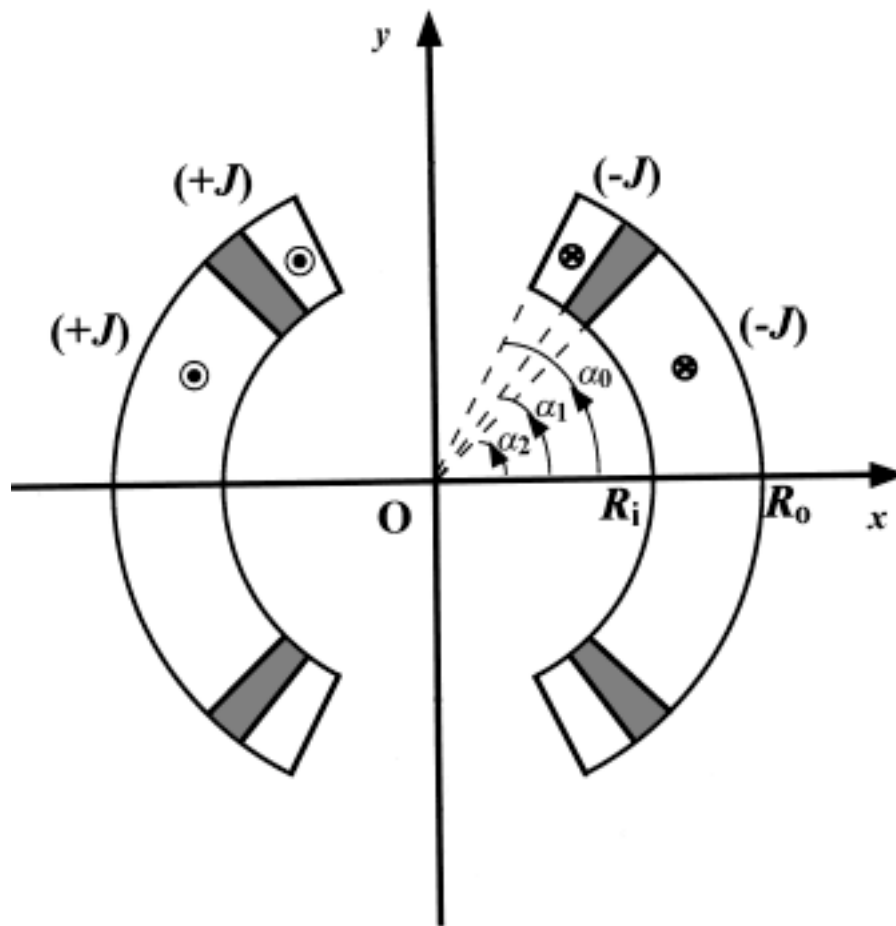
Multiple-Layer Coil

- The strength of the main field component can be raised by using multiple-layer coils.

- Example: for a two-layer dipole coil

$$B_1 = \frac{2\mu_0 J_{\text{in}}}{\pi}\left(R_{\text{o}}^{\text{in}} - R_{\text{i}}^{\text{in}}\right)\sin\left(\alpha_0^{\text{in}}\right)$$

$$+ \frac{2\mu_0 J_{\text{out}}}{\pi}\left(R_{\text{o}}^{\text{out}} - R_{\text{i}}^{\text{out}}\right)\sin\left(\alpha_0^{\text{out}}\right)$$

Angular Wedges

• Angular wedges can ne implemented into the coil, to better approximate $\cos\theta$ $\cos 2\theta$ current distribution and eliminate undesirable higher-order multipole field coefficients.

• In theory, p wedges in a dipole coil quadrant offer enough free parameters to set to zero up to $(2p+1)$ coefficients.
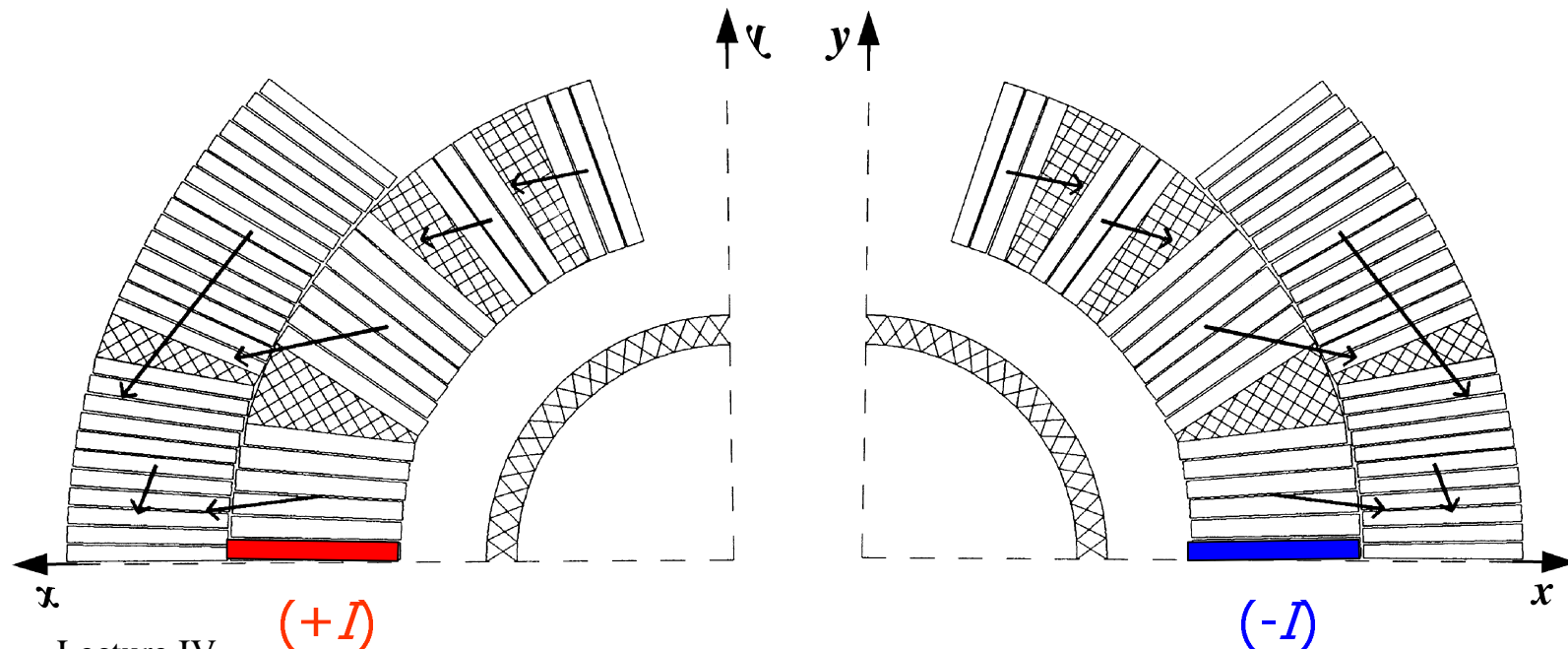
Practical Coils (1/3)
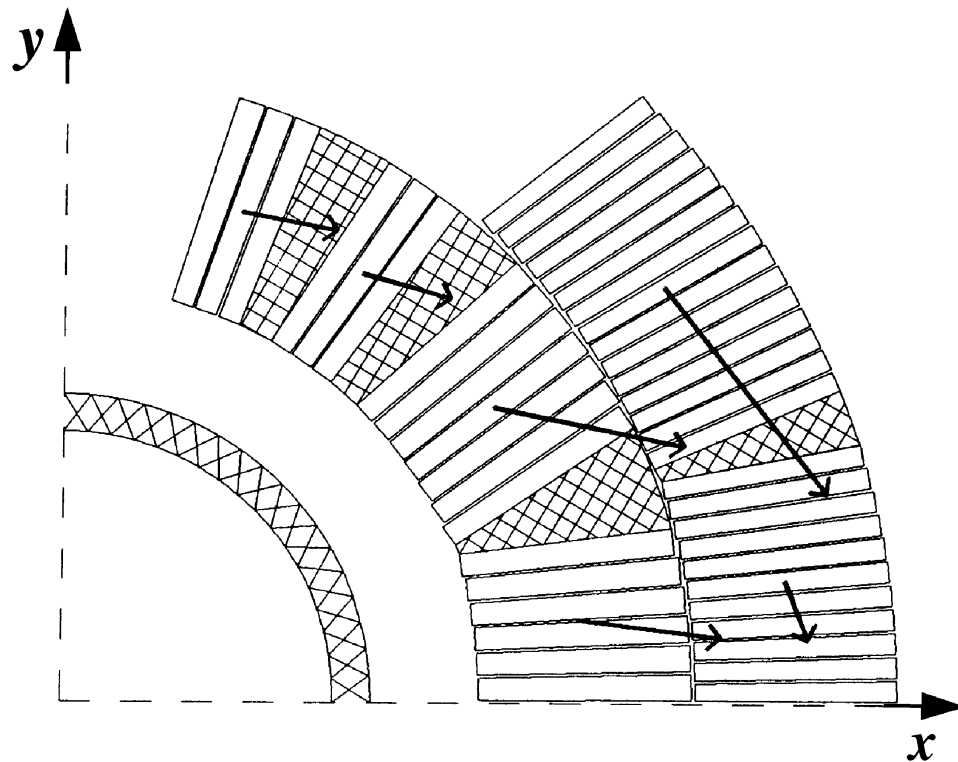
SSC Arc Dipole Magnet Coil Layout
(Courtesy R. Gupta)

- In practice, the cylindrical shells are realized by stacking slightly-keystoned conductors into an arch shape.

- The number of layers is determined by the desired field or field gradient strength.

- The number of wedges is determined by field quality requirements imposed by beam optics.

Practical Coils (2/3)

• The coil turns are formed by pairing conductors of adjacent sectors, which, due to the odd symmetry, carry currents in opposite directions.

$(+I)$ $(-I)$

Practical Coils (3/3)

- In the coil ends, the conductors are wound so as to make a U-turn while clearing enough space for beam tube insertion.

- This confers to the coil a so-called *saddle shape.*
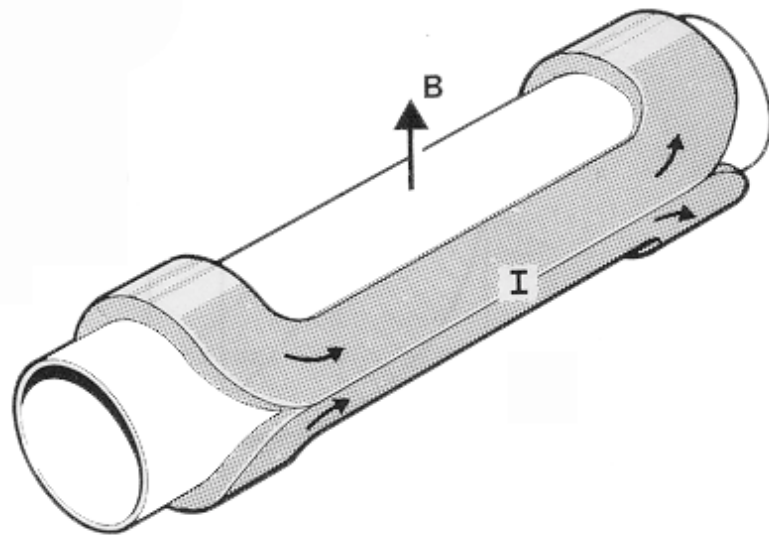
Saddle-Shape Coil Assemby
for Dipole Magnet
(Courtesy M.N. Wilson)

Winding of Quadrupole
Magnet Coil at CEA/Saclay

Pros of Cosθ Design

• The cosθ-design is the most effective design in terms of current distribution and it minimizes the volume of conductor (thereby, its costs).

• It is well proven (all large superconducting particle accelerators built up to date rely on it) and can be made to achieve very high field quality.

• R&D programs at Twenty University, in the Nertherlands, and at LBNL, in the USA, have demonstrated the feasibility of Nb$_3$Sn dipole magnets with fields in the 11-to-13.5-T range.

Cons of Cosθ Design (1/3)

- The cosθ-design has two main drawbacks
  - accumulation of transverse stress over midplane conductors,
  - difficulty of designing and manufacturing coil ends.

- These issues are particularly troublesome when using Nb$_3$Sn cables.

Lorentz Stress Accumulation

- Due to the Lorentz force distribution, there is a stress accumulation in the azimuthal direction, which results in high transverse pressures on the midplane conductors of coil assemblies.

σ_θ

σ (MPa)

High Stress Area
(~150 MPa)
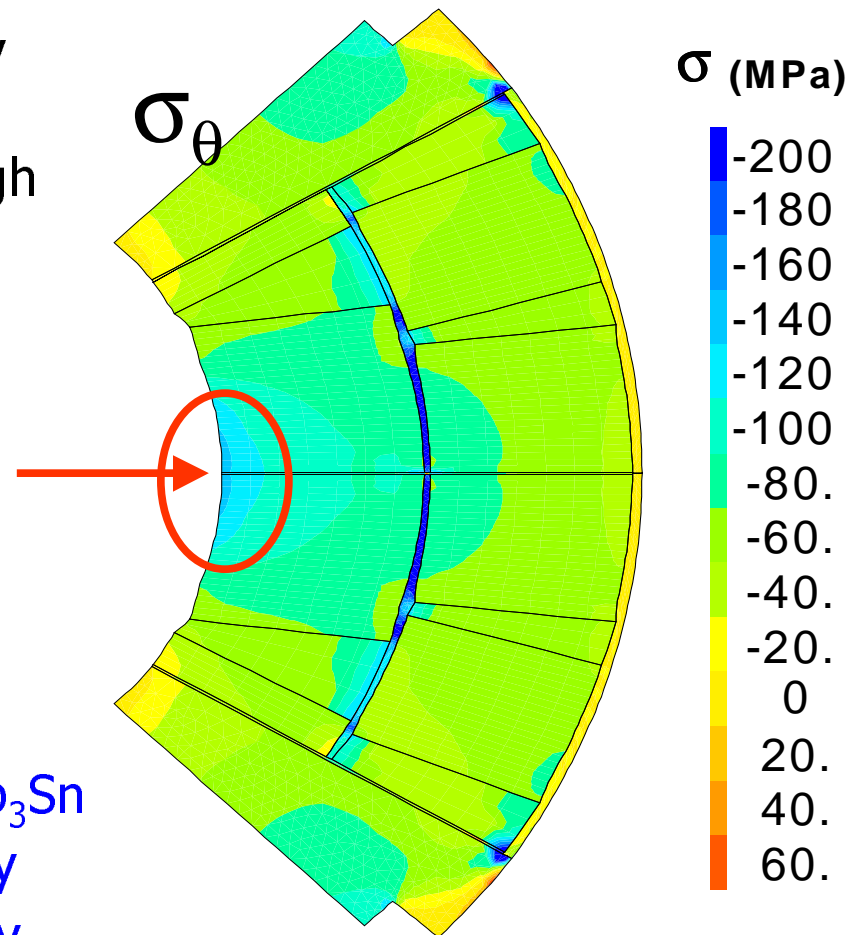
Azimuthal Stress Distribution in a Nb_3Sn Quadrupole Magnet Coil Assembly Under Development at CEA/Saclay (Courtesy C. Gourdin)

Lecture IV

41

# Coil End Design (1/2)

Winding Test at CEA/Saclay
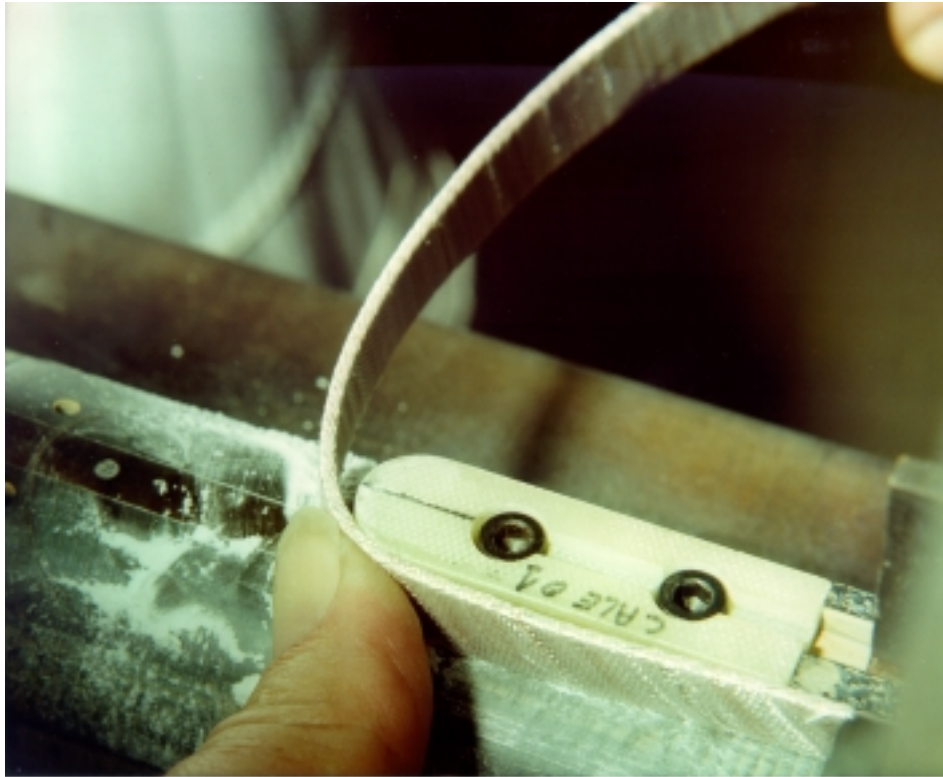
• In the coil ends, the conductors are bent sharply with small radii or curvature.

• Such bending cannot be applied to reacted Nb_3Sn cables, and imposes to rely on a "wind & react" process.

Lecture IV

42

Coil End Design (2/2)

- Furthermore, it is desirable to position properly the conductors so as to minimize the risks of motion during energization.

- This calls for the use of precisely machined (thereby expansive) end spacers.
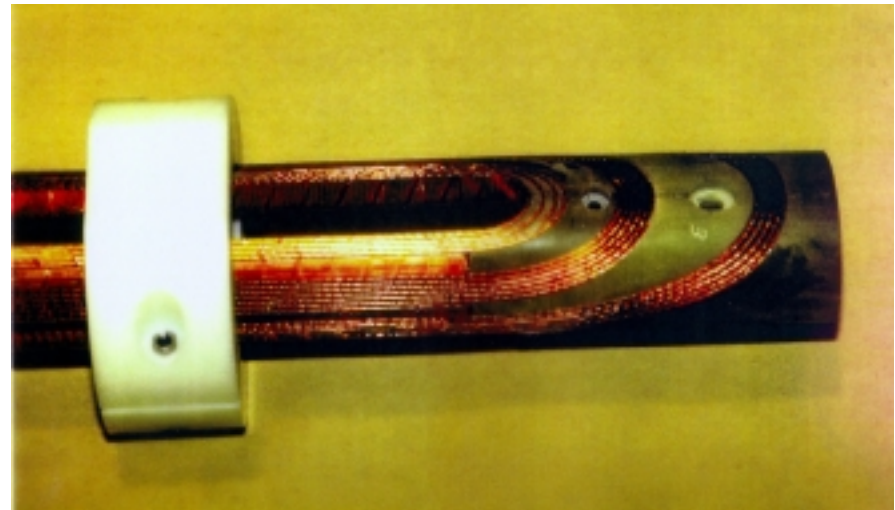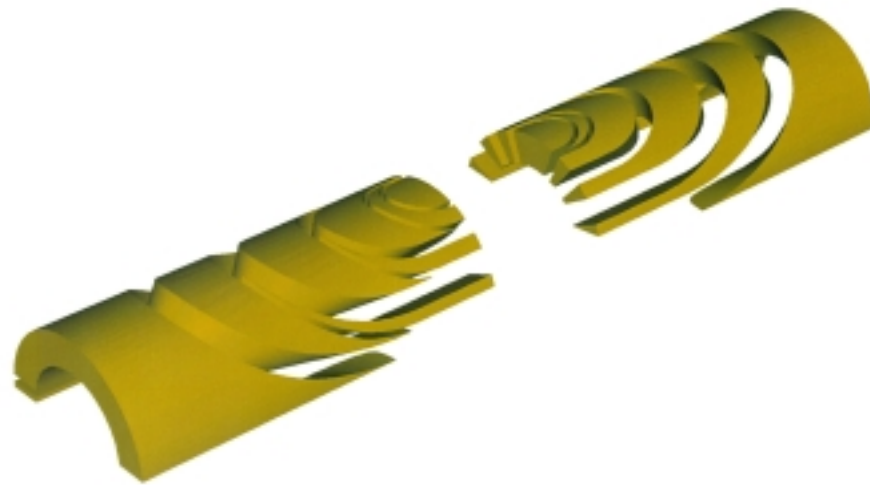
Coil Ends of LHC Dipole Magnets (Courtesy D. Perini)

- Note that the end spacers are also needed for field quality reasons.

Cosθ-Design Perspectives

- As already mentioned, for the past 20 years, the cosθ-design has been the working horse of NbTi accelerator magnet developers.

- Encouraging results have been obtained on short magnet models relying on Nb_3Sn cables, which show that it is worth pursuing in this direction.

- However, the inherent limitations mentioned above, and the fact that, for Nb_3Sn cables, one must rely on a "wind & react" process, justify that one looks for alternative designs.

Contents

- **Notations**
- **Field Computations for Simple Current Line Distributions**
- **Cosθ and Cos2θ Coil Designs**
- **Iron Yoke Contribution**
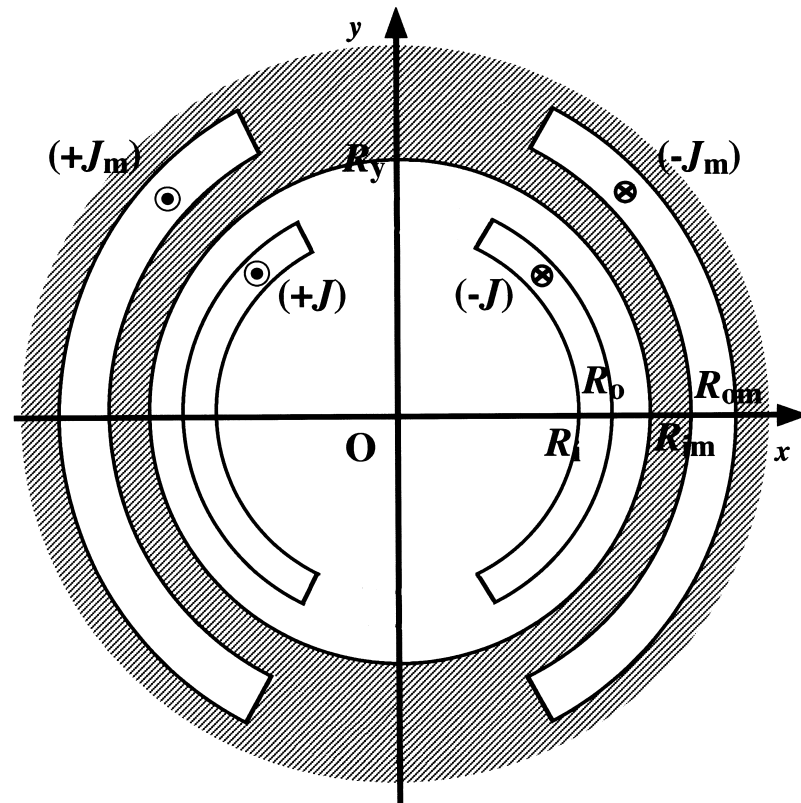- **Operating Current Margin**
- **Other Designs**

Iron Yoke (1/3)
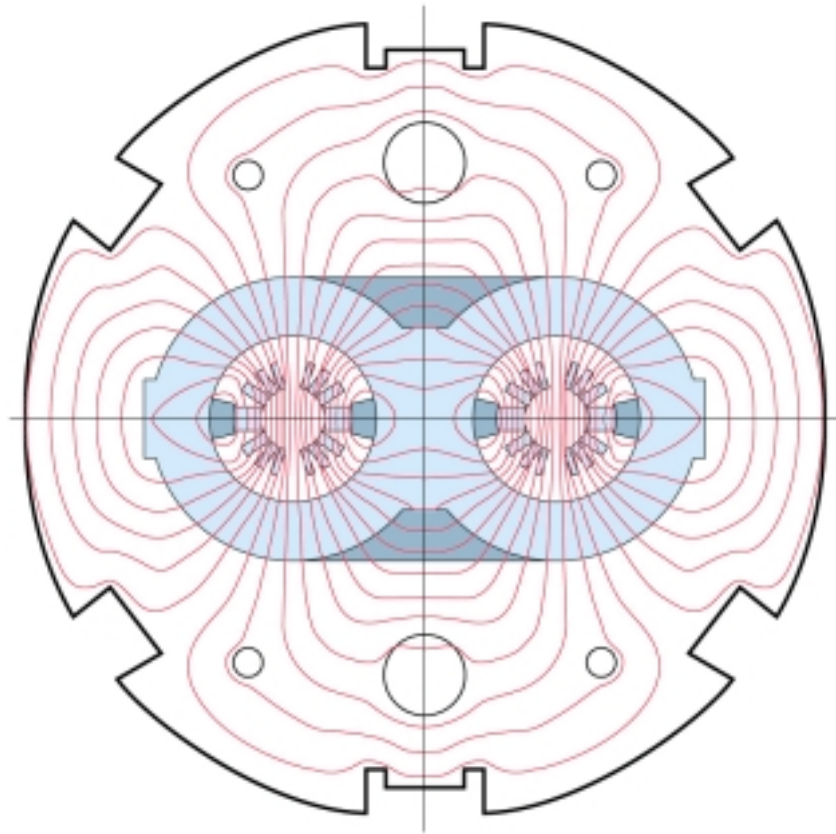
Twin-Aperture LHC Dipole
Magnet Field Lines

- The coils of accelerator magnets are usually surrounded by a cylindrical iron yoke.

- This iron yoke provides a return path for the magnetic flux and enhances the central field or field gradient.

Iron Yoke (2/3)

• For a cylindrical shell located within an iron yoke of inner radius, R_y, the normal $2n$-pole field coefficients with iron, $B_n^{\text{w.y.}}$ are given by

$$\frac{B_n^{\text{w.y.}}}{B_n^{\text{w/o.y.}}} = 1 + \frac{\mu - 1}{\mu + 1}\left(\frac{R_o R_i}{R_y^2}\right)^n$$

where $B_n^{\text{w/o.y.}}$ designate the coefficients produced by the shell alone in free space.

47

Iron Yoke (3/3)

- The previous equation shows that, the smaller the yoke inner radius, the larger the enhancement.
- However, there are two limitations on how close the iron can be brought to the coils
  - room must be left for support structure *(see lecture on mechanical design)*,
  - iron saturates for fields above 2 T, resulting in undesirable distortions *(see lecture on field quality)*.

Contents

- **Notations**
- **Field Computations for Simple Current Line Distributions**
- **Cosθ and Cos2θ Coil Designs**
- **Iron Yoke Contribution**
- **Operating Current Margin**
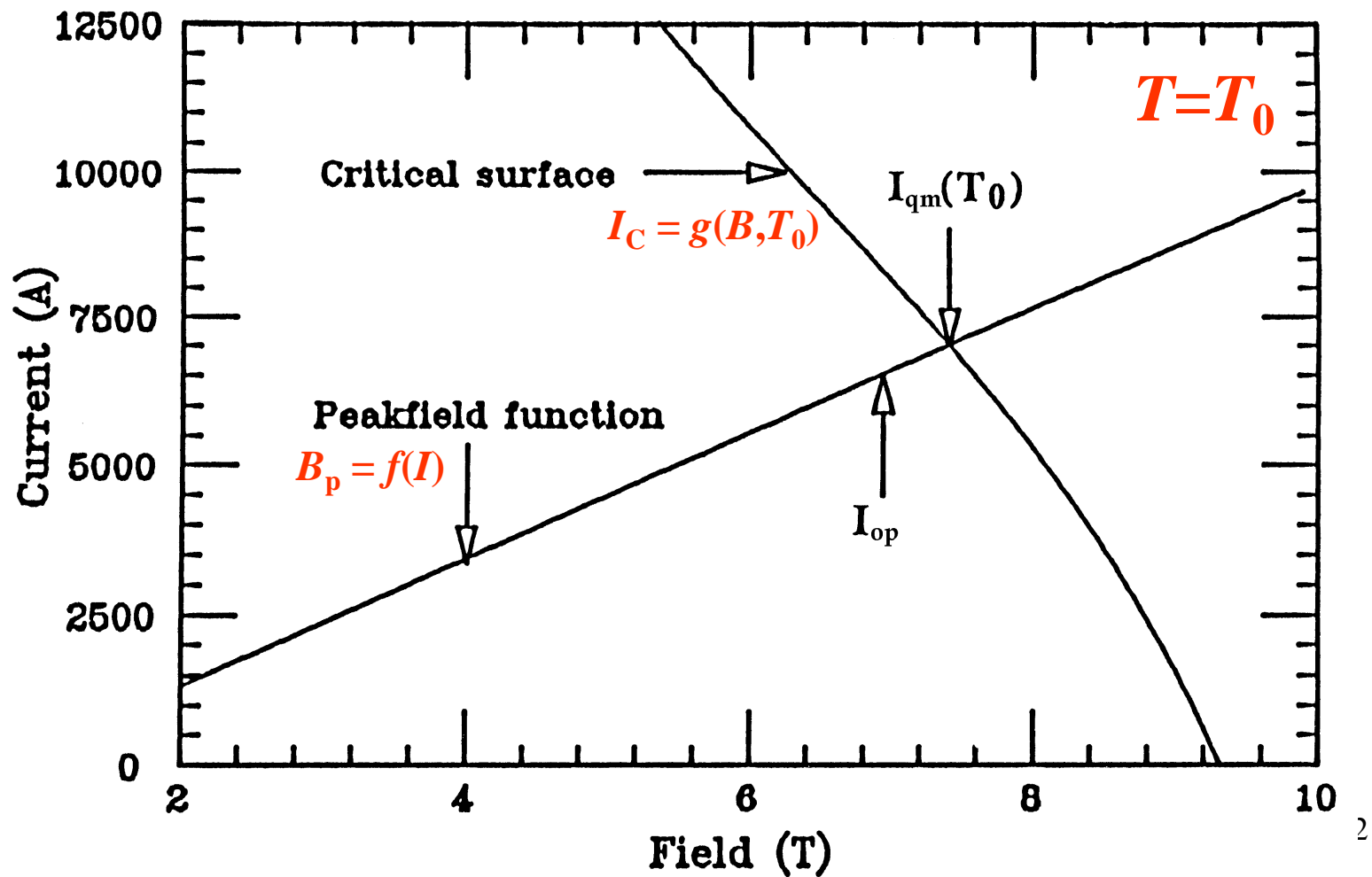- **Other Designs**

Maximum Quench Current (1/3)

• The ultimate performance of a superconducting magnet is determined by the critical current of its conductor at the operating temperature and magnetic flux density.

• The magnetic flux density to which the conductor is exposed is non-uniform over the magnet coil, but the limit is set by the section where the magnetic flux density is the highest.

Maximum Quench Current (2/3)

- Let $B_p = f(I)$ designate the peak magnetic flux density on the coil as a function of supplied current, I, and let $I_C = g(B, T_0)$ designate the supposedly known cable critical current as a function of applied magnetic flux density, B, and operating temperature, T_0.

- The intersection between these two curves determines the maximum quench current of the magnet at T_0, $I_{qm}(T_0)$.

Maximum Quench Current (3/3)

$T=T_0$

Critical surface

$I_C = g(B,T_0)$

$I_{qm}(T_0)$

Peakfield function

$B_p = f(I)$

I_{op}

Current (A)

Field (T)

Operating Current Margin

- In practice, magnets must be operated below I_{qm} to ensure that the entire coil is in the superconducting state and to limit the risks of premature quenching.

- Let I_{op} designate the operating current. Then, the operating current margin of the magnet, m_I, is defined as

$$m_I = 1 - \frac{I_{op}}{I_{qm}(T_0)}$$

Current Margin Specifications

• For accelerator magnets, which are produced in large quantities and where the volume of superconductor must be minimized to reduce costs, the operating current margin can be as small as 10%.

• For large detector magnets, where reliability is a big issue, the current margin can be in excess of 50%.

Contents

- **Notations**
- **Field Computations for Simple Current Line Distributions**
- **Cosθ and Cos2θ Coil Designs**
- **Iron Yoke Contribution**
- **Operating Current Margin**
- **Other Designs**

Other Designs

• Most other accelerator magnet designs, which have been or are being developed, try to address the perceived weaknesses of $\cos\theta$ design, *i.e.*,

– management of Lorentz forces,
– complexity of coil ends.

Block Design (1/2)

• The conductors are wound into precisely machined grooves of support structure.

• Each conductor block is supported individually, and the conductors are parallel to field lines (which cut down interstrand coupling currents).
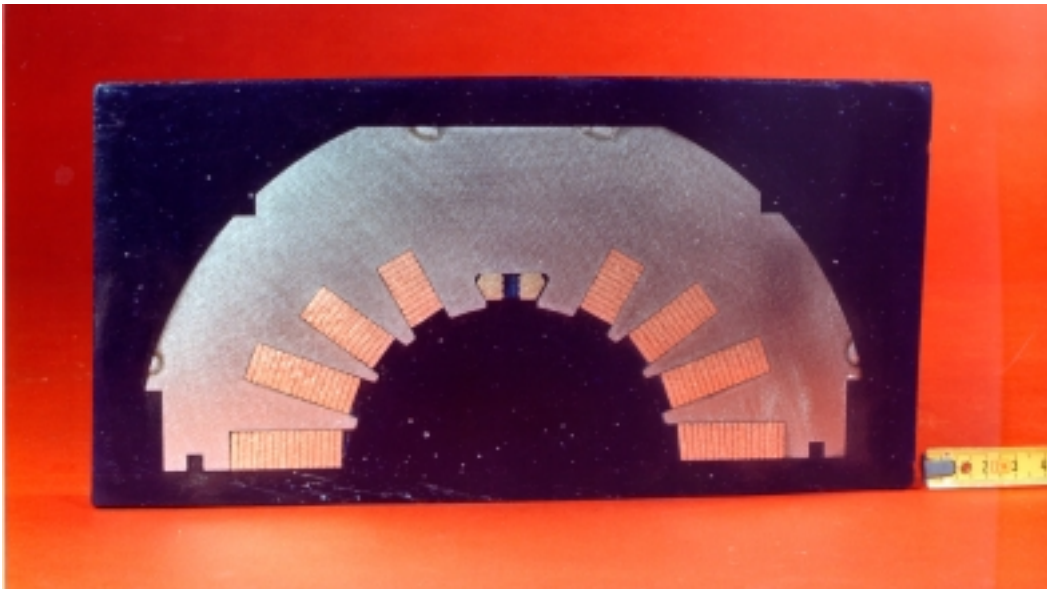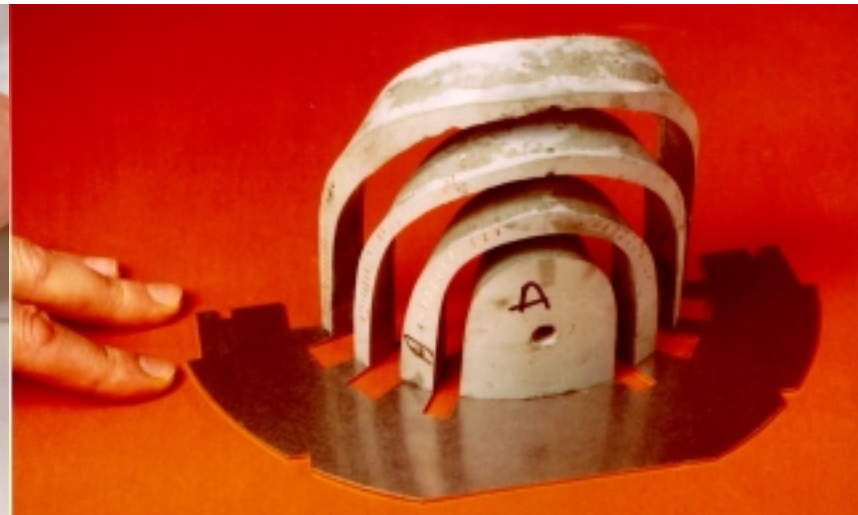

• 100-mm-aperture, HERA-type dipole magnet model developed by J. Pérot at CEA/Saclay.

• Two models have been built and cold-tested in 1981 and have reached short sample limit with limited training (5 and 7 quenches).

Block Design (2/2)

- Manufacturing process is cumbersome.
- Design cannot be extrapolated to small apertures for the fingers extending between conductor blocks would become too small.
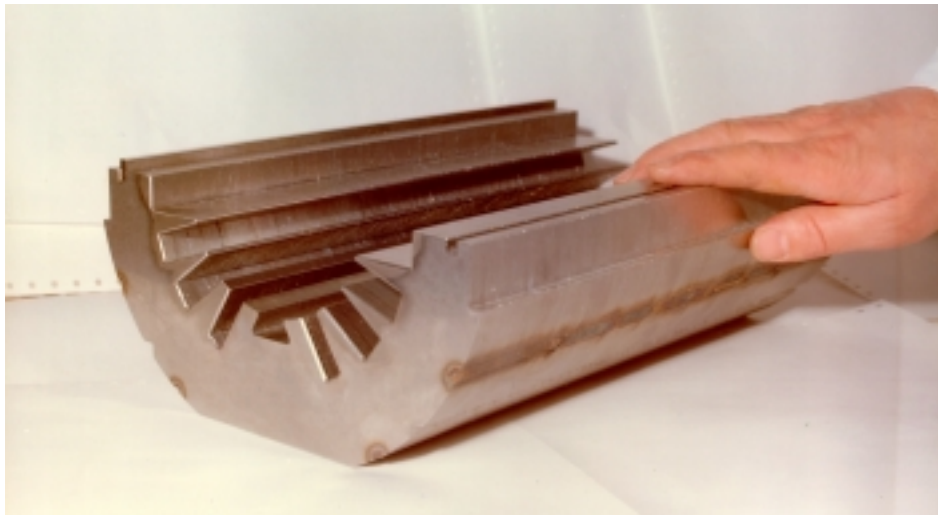

Laminated Support Structure
Lecture IV (Courtesy J. Pérot)

Coil End Spacer
(Courtesy J. Pérot) 58

"Window-Frame" Design

- KEK has built and cold tested in the early eighties a 1-m-long, 60-mm-aperture dipole magnet model made up of eigth double-pancake coils assembled in a "window-frame" configuration.

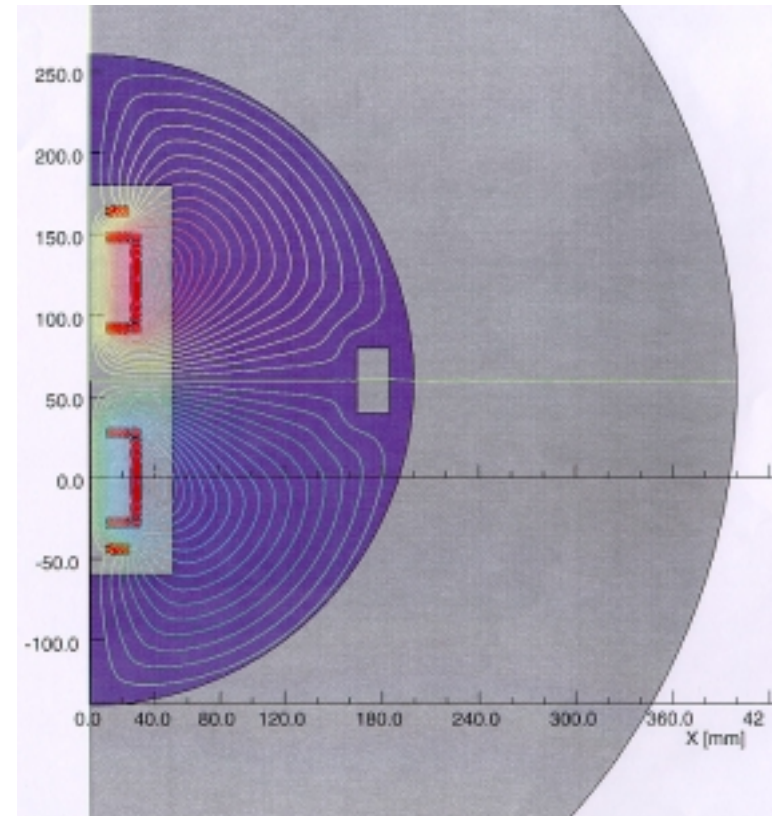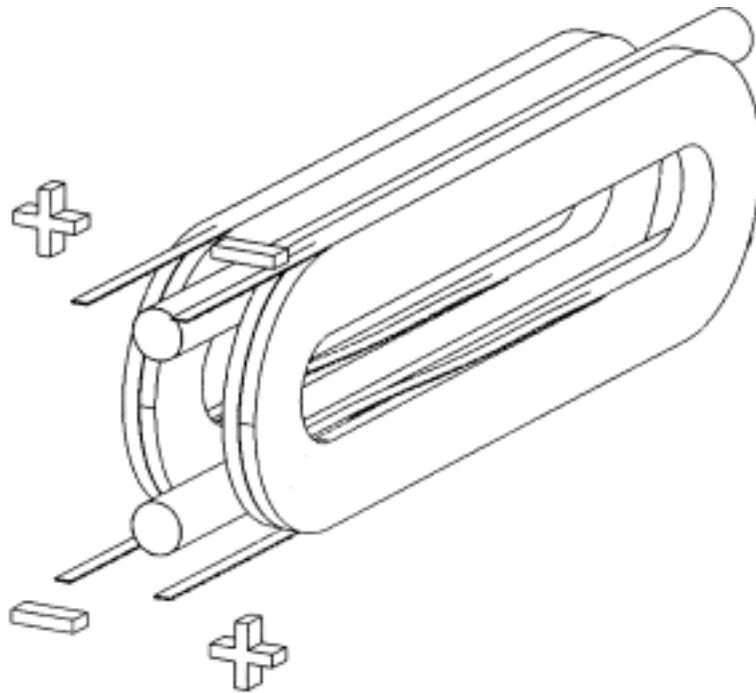- The magnet (which relied on NbTi cables) reached a maximum field of 9.3 T at 1.8 K in a few training steps.
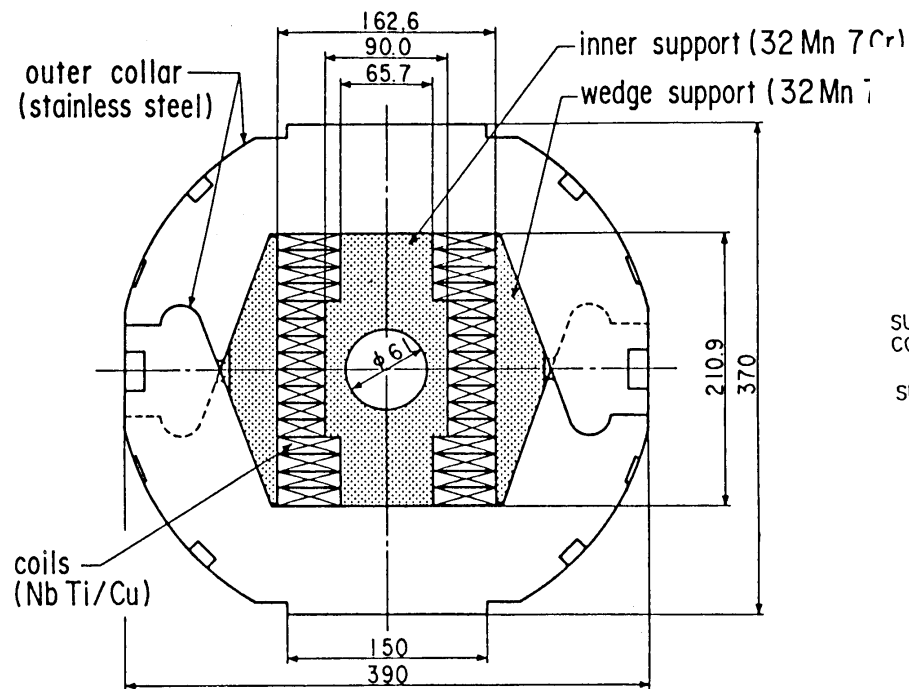
Lecture IV
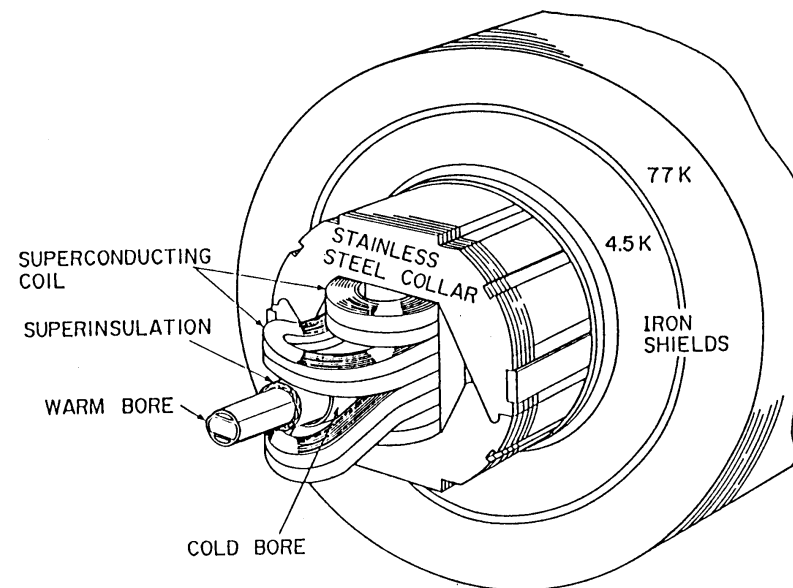
(Courtesy T. Shintomi)

"Common Coil" Design (1/4)

- In 1996, R. Gupta has proposed an innovative twin-aperture dipole magnet design based on pairs of parallel racetrack-type coils fed with currents of opposite directions.


Lecture IV   **(Courtesy R. Gupta)**

"Common Coil" Design (2/4)

• The "common coil" design offers at least two advantages
  – the radii of curvature of coil ends may be large enough to allow manufacturing by the "react and wind" process when using Nb_3Sn conductors,
 – the overall mechanical design is simpler.

"Common Coil" Design (2/4)

• LBNL has built a 1-m-long model made up of two pairs of Nb_3Sn coils with a spacing of 25 mm (the coils were produced by a "wind and react" process).

Common-Coil Design Dipole Magnet Model Built at LBNL
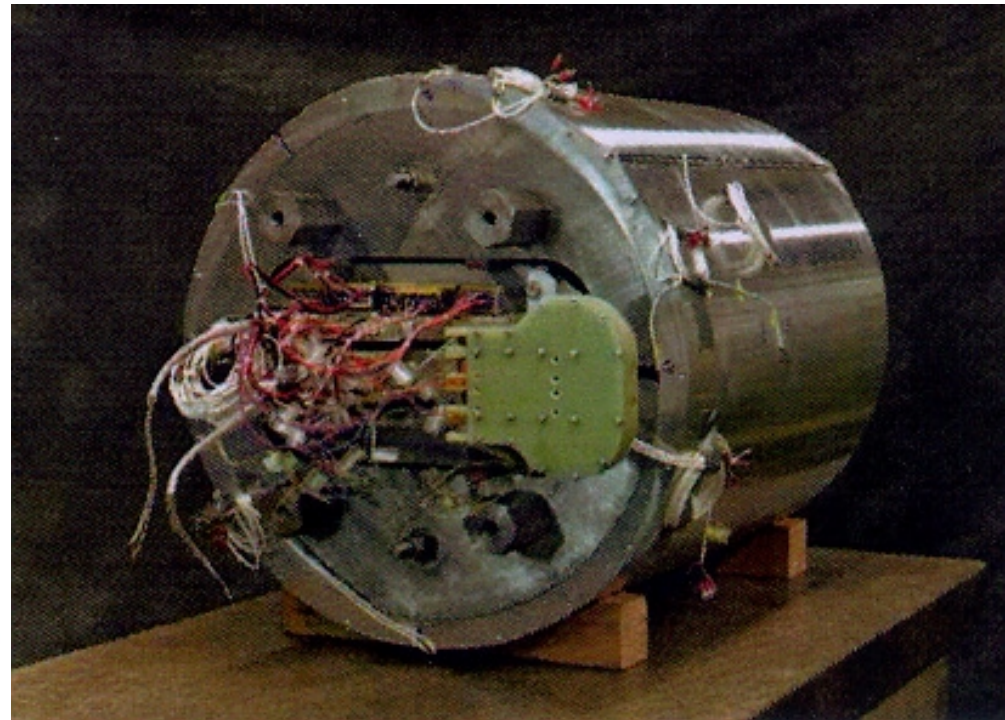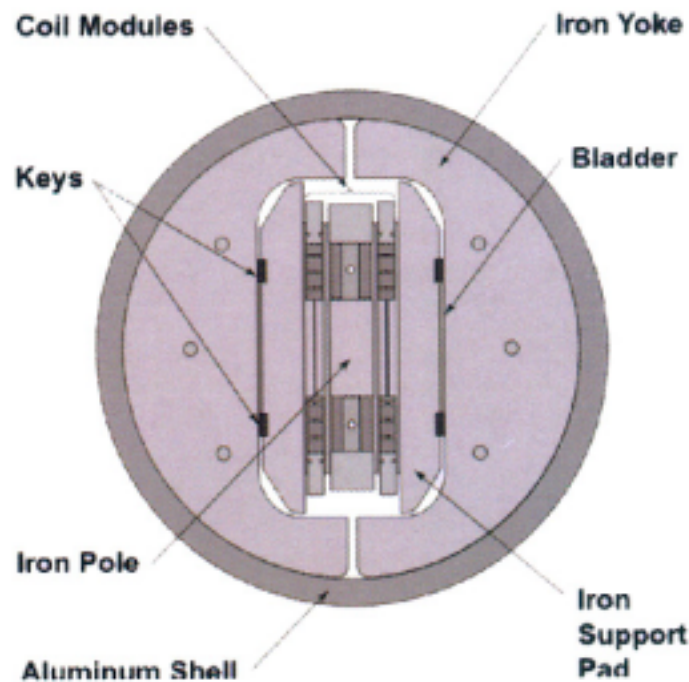
"Common Coil" Design (3/4)

• The model was cold-tested earlier this year (2001) and has reached a record field of 14.7 T at 4.2 K.
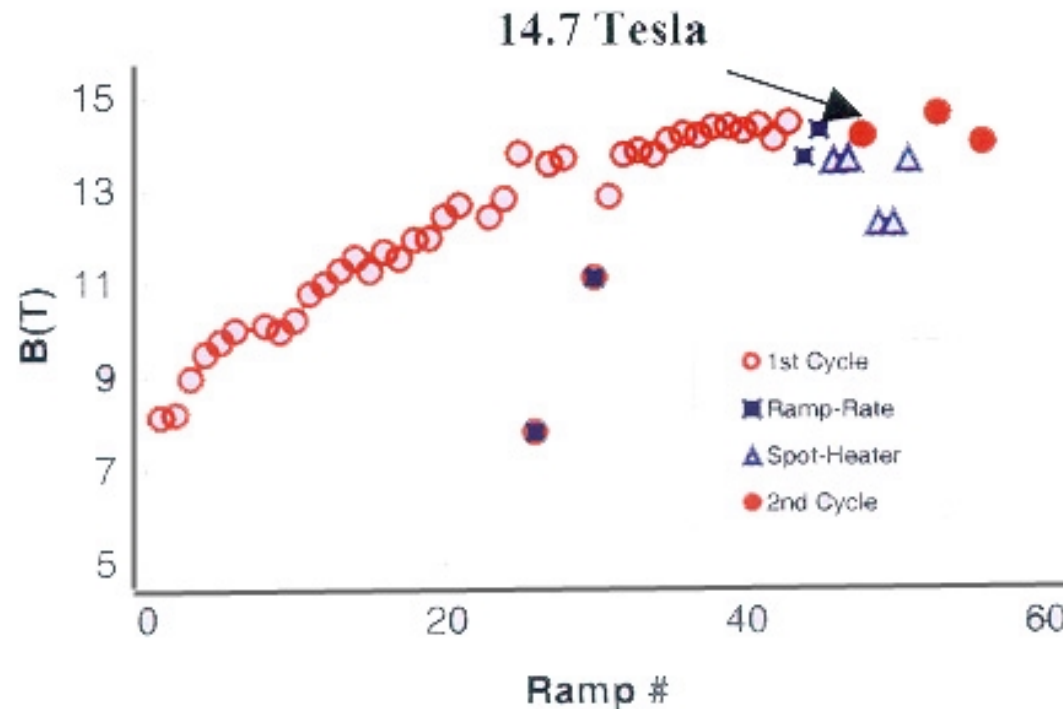

Quench Plot of LBNL
Common-Coil Design Dipole Magnet Model

"Common Coil" Design (4/4)

• This first result is very promising.

• However, far more work is needed to validate the "common-coil" design, to demonstrate its suitability to high-energy accelerators (especially in terms of field quality), and to assess production costs.

• R&D programs on common-coil magnets have now been undertaken at other US national laboratories.

• In particular, FNAL is investigating the "react and wind" route.

"Stress Management" Design (1/2)
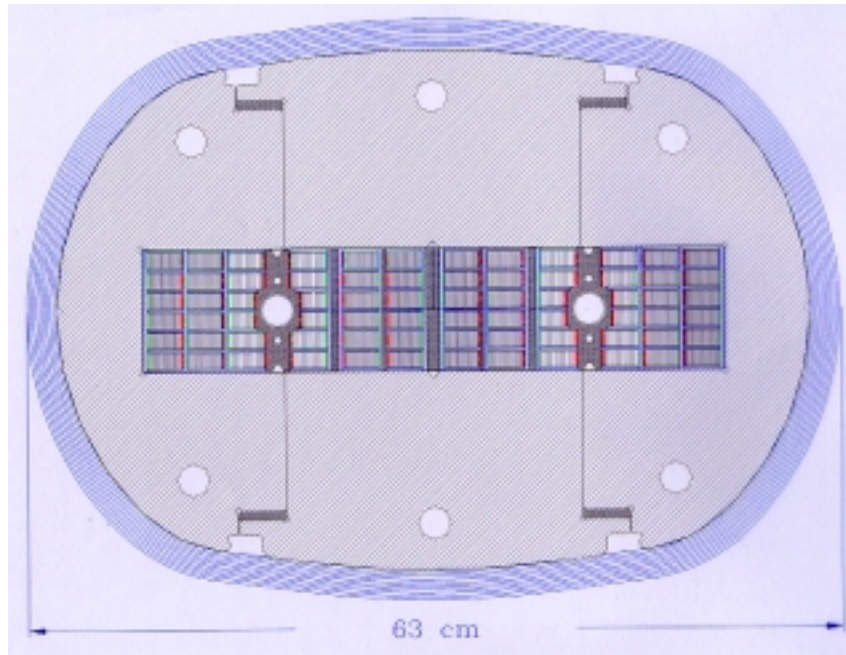
(Courtesy P. McIntyre)

• Texas A&M University has developed a dual-dipole magnet design concept, where the conductors are divided into blocks to limit transverse stresses to less than 100 MPa.

Lecture IV
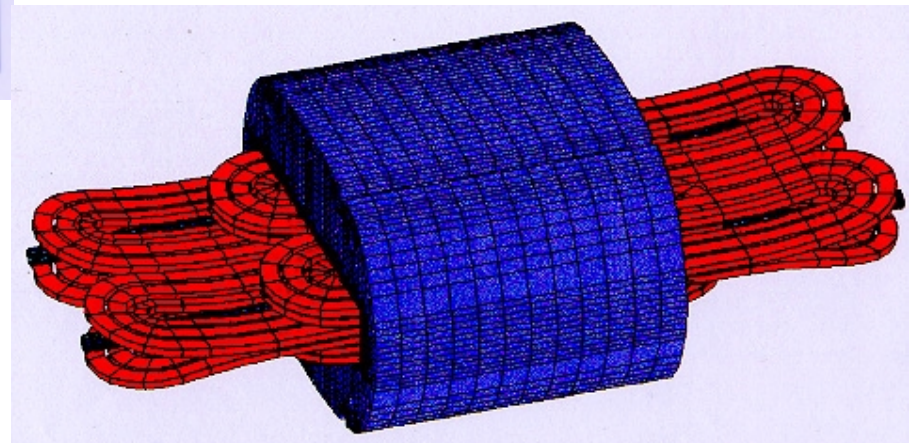
"Stress Management" Design (2/2)
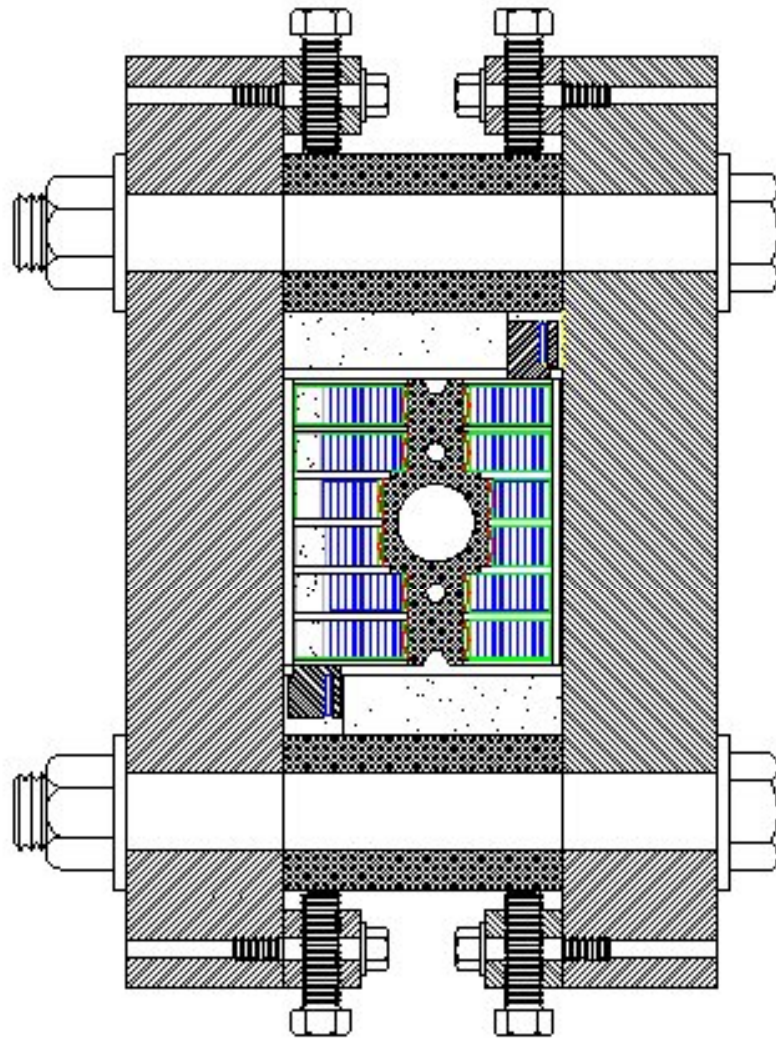
- A single-aperture NbTi model has been built and cold tested in late 2000/early 2001.

- The model has reached a maximum field of 6.6 T at 4.2 K (~ 98% of short sample limit) in a few training steps.

TAMU Dipole
Magnet Model
(Courtesy
P. McIntyre)

Transmission Line Design (1/4)
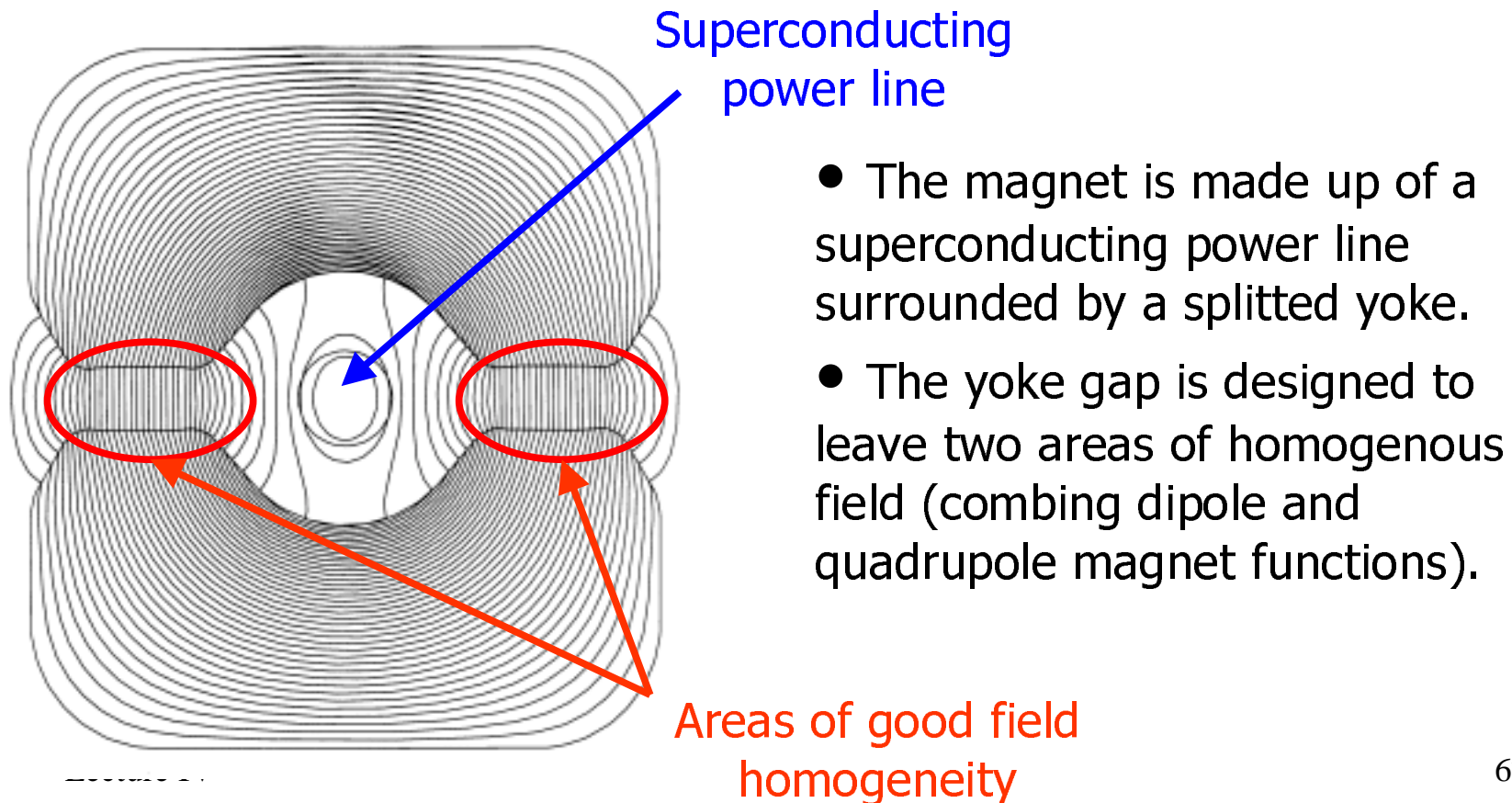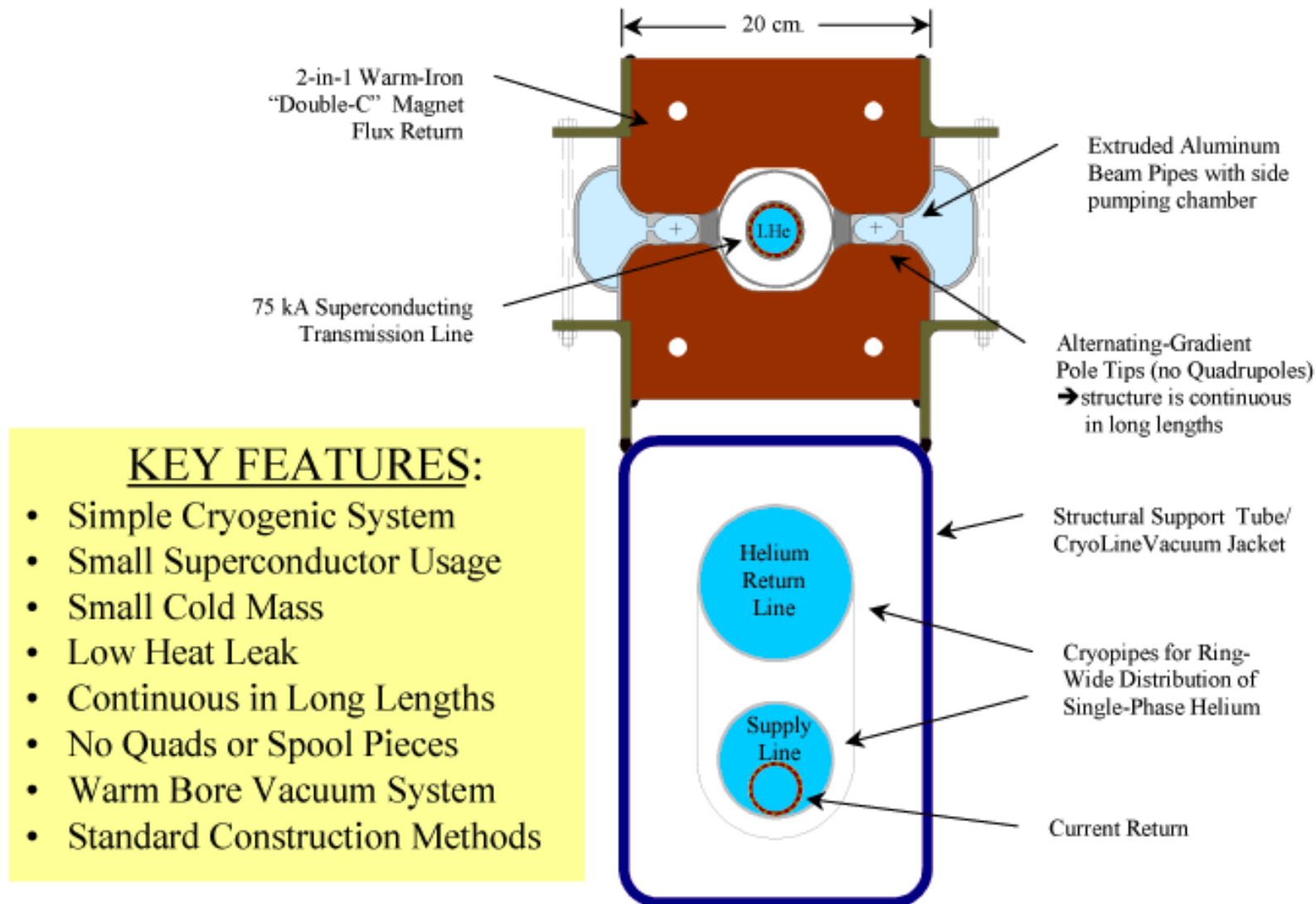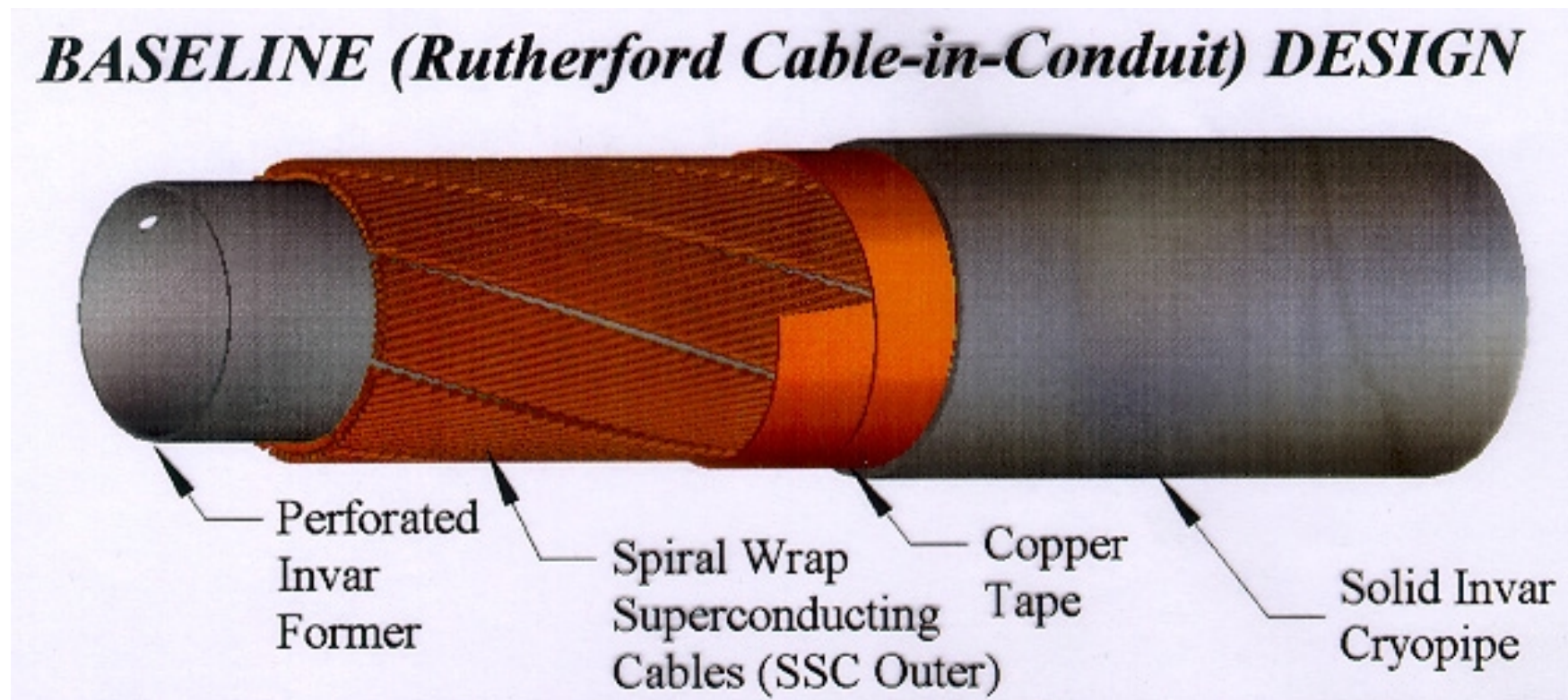
- FNAL has developed a "transmission line" magnet design as a low-field (2 T), and possibly low-cost, option for VLHC.

Superconducting power line

Areas of good field homogeneity

- The magnet is made up of a superconducting power line surrounded by a splitted yoke.

- The yoke gap is designed to leave two areas of homogenous field (combing dipole and quadrupole magnet functions).

Transmission Line Design (2/4)

20 cm.

2-in-1 Warm-Iron "Double-C" Magnet Flux Return

Extruded Aluminum Beam Pipes with side pumping chamber

LHe

75 kA Superconducting Transmission Line

Alternating-Gradient Pole Tips (no Quadrupoles) ➔ structure is continuous in long lengths

KEY FEATURES:
- Simple Cryogenic System
- Small Superconductor Usage
- Small Cold Mass
- Low Heat Leak
- Continuous in Long Lengths
- No Quads or Spool Pieces
- Warm Bore Vacuum System
- Standard Construction Methods

Structural Support Tube/ CryoLineVacuum Jacket

Helium Return Line

Cryopipes for Ring-Wide Distribution of Single-Phase Helium

Supply Line

Current Return

Transmission Line Magnet (3/4)

BASELINE (Rutherford Cable-in-Conduit) DESIGN

Perforated Invar Former

Spiral Wrap Superconducting Cables (SSC Outer)

Copper Tape

Solid Invar Cryopipe

Transmission-Line Design (4/4)

- A 17-m-long demonstration loop has been built at Fermilab and has been excited up to 100 kA.

- The next step is to build, a 60-m-long magnet section.

Transmission-Line Test Loop at FNAL